A model for hierarchical patterns under mechanical stresses

F. Corson [a]; H. Henry [b]; M. Adda-Bedia [a]

[a] Laboratoire de Physique Statistique, École Normale Supérieure, CNRS, 75231 Paris Cedex 05, France [b] Physique de la Matière Condensée, École Polytechnique, CNRS, 91128 Palaiseau, France

PLEASE SCROLL DOWN FOR ARTICLE

Taylor & Francis
Taylor & Francis Group

A model for hierarchical patterns under mechanical stresses

F. Corson[a], H. Henry[b]* and M. Adda-Bedia[a]

[a]*Laboratoire de Physique Statistique, École Normale Supérieure, CNRS, 24 rue Lhomond, 75231 Paris Cedex 05, France;* [b]*Physique de la Matière Condensée, École Polytechnique, CNRS, rte de Saclay, 91128 Palaiseau, France*

We present a model for mechanically-induced pattern formation in growing biological tissues and discuss its application to the development of leaf venation networks. Drawing an analogy with phase transitions in solids, we use a phase field method to describe the transition between two states of the tissue, e.g. the differentiation of leaf veins, and consider a layered system where mechanical stresses are generated by differential growth. We present analytical and numerical results for one-dimensional systems, showing that a combination of growth and irreversibility gives rise to hierarchical patterns. Two-dimensional simulations suggest that such a mechanism could account for the hierarchical, reticulate structure of leaf venation networks, yet point to the need for a more detailed treatment of the coupling between growth and mechanical stresses.

Keywords: mechanical instabilities; phase field; numerical modeling; pattern dynamics

1. Introduction

A broad range of patterns in nature are induced by mechanical forces. While the most well understood examples are found in physical phenomena, e.g. in solids, fracture [1], wrinkling [2], delamination [3], or localized deformation [4], it is increasingly becoming appreciated that mechanical forces are also essential in the morphogenesis of living organisms. In the simplest case, biological tissues can undergo mechanical instabilities as a result of inhomogeneous growth [5,6]. More broadly, the importance of the mechanical and adhesion properties of cells in morphogenesis [7] and the ability of mechanical forces to act as a signal in growing tissues and organisms [8–10] suggest that the interplay between mechanical forces and biochemical factors has a central role in development.

An illustration of these ideas can be found in recent investigations of the structure of leaf venation networks [11]. The standard model for vein formation involves the transport of the plant hormone auxin [12]: auxin circulates through the leaf, with the leaf base acting as a sink; as the leaf develops, auxin flow becomes progressively concentrated along preferential paths, which mark the location of future veins. This model has received ample experimental support (see e.g. [13]), yet it fails to explain

*Corresponding author. Email: herve.henry@polytechnique.edu

certain aspects of leaf venation, such as the presence of closed loops. Simulations of auxin transport generally give rise to tree-like structures [14], a typical property of diffusion-limited growth processes [15]. In contrast, it has been noted that the reticulate structure of venation networks is very similar to that of crack patterns, suggesting the possibility that the differentiation of leaf veins could be governed by mechanical stresses [11]. The inner tissues of the leaf, where the veins form, are subjected to compressive stresses by the epidermis, and one of the earliest signs of vein differentiation is the elongation of vascular cells [16], which could release the compressive stresses in their vicinity, providing a feedback between differentiation and the mechanical state of the tissue.

In this article, we develop a theoretical approach to study the formation of patterns induced by mechanical stresses in biological tissues. Of particular interest is the fact that these tissues are growing as the patterns form. We show how growth can be the driving force that causes the formation of new structures, and how the history of their formation can be reflected in their organization. Let us emphasize that this study mainly aims at demonstrating possible effects of mechanical stresses, and that the approach developed here would have to be integrated with biochemical mechanisms in a more complete model.

Stated in general terms, the patterning mechanism we consider is the following: compressive stresses imparted on a tissue cause it to switch to a 'collapsed' state occupying a smaller volume, whereby the compression is released. In the case of leaf venation, this transition describes the differentiation of veins, and the collapsed state refers to the elongated vascular cells. An analogy can be made with the behavior of solid foams, which exhibit localized deformation upon compression [4]. Our model is not explicitly constructed according to this analogy. Instead, we consider the initial and collapsed states of the tissue as two phases of a continuous medium, which we describe using a phase field method. However, the response of this two-phase medium is analogous to that of a non-linear elastic material, and can be analyzed with reference to the behavior of such materials.[1]

In what follows, we first present our model in a one-dimensional setting. We define a minimal model, amenable to analytical treatment, that implements the patterning mechanism described above. We consider a layered system, in which the tissue is coupled to a rigid substrate, which could represent a stiffer tissue such as the epidermis of plant leaves. Stresses are induced by a mismatch between the two layers, which can occur as a result of differential growth. If the transition between the two states of the tissue is reversible, regular patterns are obtained, in which domains of collapsed and uncollapsed tissue alternate. If, instead, the transition to the collapsed state is made irreversible to model tissue differentiation, hierarchical patterns are obtained.

When turning to two-dimensional systems, the tensorial nature of mechanical fields comes into play, and a much greater variety of behaviors are possible. Rather than to attempt a systematic exploration, we present a few illustrative examples of the patterns that can be obtained. In particular, we show that anisotropic collapse, which could describe the elongation of vascular cells in plant leaves, produces reticulate patterns comprised of interconnected stripes of collapsed tissue. Our simulation results suggest that hierarchical, reticulate patterns might be obtained when irreversibility is introduced. However, in the simple model presented here, these

patterns are disrupted by strong residual stresses that develop in the vicinity of growing collapsed regions. We suggest that a more satisfactory model would require a more detailed description of the interplay between mechanical stresses and growth. We also contrast our model with a similar approach presented in [17].

2. One-dimensional model

In this section, we present our modeling approach in the context of a one-dimensional system. We consider a tissue that can exist in two states, an 'initial' state and a 'collapsed' state that has a smaller volume. Transition to the collapsed state is triggered by compressive stresses, and releases the compression. While, in general, the two states of the tissue could differ in their stiffness (the collapse could be due to the transition to a softer state), we assume that they only differ in their rest configurations (the collapsed state has a smaller volume at rest). In the case of leaf veins, the initial and collapsed states of the tissue represent the undifferentiated and vascular tissues, respectively, and the change in rest configuration corresponds to the elongation of vascular cells as they differentiate. The tissue is described as a continuous medium, and its two states as two 'phases', using a phase field model.

The phase field approach, used here in the context of mechanically induced pattern formation [17], was first introduced to describe the growth of a solid in a liquid [18–21] (reviewed in [22,23]) and has later proved to be a powerful tool to describe free boundary problems in fluid flows [24,25] and solid-solid phase transitions in alloys [26,27]. This is especially the case in 3D, where interface tracking methods are extremely difficult to implement [28,29]. Our model is similar to those developed for fracture in [30–34] and for solid-solid phase transitions in [26,27], which comprise phases having different mechanical properties.

A continuously varying auxiliary field ϕ is introduced to indicate the local state of the tissue, with the convention that $\phi = 0$ corresponds to the initial state, and $\phi = 1$ to collapsed regions. The behavior of the system, i.e. both its deformations and the transitions between the two states, is assumed to be governed by an energy functional $E\{\phi, u\}$, where u is the displacement field. While this is natural for a physical system, it may seem rather arbitrary for a biological one. However, we will see that the resulting behavior is sufficiently general. The evolution of the system is assumed to be quasi-static, i.e. at any given time it is in a state of equilibrium that minimizes E, and satisfies the equilibrium equations

$$\frac{\delta E}{\delta u} = 0 \tag{1}$$

$$\frac{\delta E}{\delta \phi} = 0. \tag{2}$$

For a one-dimensional system, the energy E is defined by

$$E = \int \left[\frac{D}{2} (\partial_x \phi)^2 + e(\phi, \epsilon) + f(\phi) \right] \mathrm{d}x. \tag{3}$$

The first term in the integral is a squared gradient term, which penalizes sharp variations in the phase field. e is the density of elastic energy, which depends on the phase and on the strain $\epsilon = \partial_x u$. $f(\phi)$ is a potential that, together with the coupling between ϕ and ϵ through e, governs the behavior of the phase field. Assuming that both phases (treated as linear elastic) have the same elastic modulus μ and differ only in their rest configuration, the energy defined by Equation (3) takes the form

$$E = \int \left[\frac{D}{2}(\partial_x \phi)^2 + \frac{\mu}{2}(\epsilon - \epsilon_r(\phi))^2 + f(\phi) \right] dx, \qquad (4)$$

where the rest configuration is given by

$$\epsilon_r(\phi) = h(\phi)\epsilon_{r1}. \qquad (5)$$

The function h (defined below) satisfies $h(0) = 0$ and $h(1) = 1$, and ϵ_{r1} is the rest configuration of the collapsed phase. The potential f is defined by

$$f(\phi) = \alpha h(\phi)^2 + \beta h(\phi). \qquad (6)$$

$h(\phi) = 3\phi^2 - 2\phi^3$ is chosen such that $h'(0) = h'(1) = 0$, so that uniform phases ($\phi = 0$ or $\phi = 1$) are stationary states.

Qualitatively, it can seen be from Equation (4) that under sufficient compression, the system will tend to switch to the collapsed state to lower its energy. The response of the system can be described by examining its uniform states of equilibrium (where ϕ and ϵ are uniform). In the range of parameters considered here,[2] ϕ has a unique equilibrium value for every value of the strain ϵ. Defining the critical strains

$$\epsilon_{c0} = \frac{\beta}{\mu \epsilon_{r1}}, \qquad (7)$$

$$\epsilon_{c1} = \frac{\mu \epsilon_{r1}^2 + 2\alpha + \beta}{\mu \epsilon_{r1}}, \qquad (8)$$

ϕ is equal to 0 when $\epsilon > \epsilon_{c0}$ (note that since we are considering compressive strains, ϵ and σ are generally negative), varies gradually from 0 to 1 as ϵ goes from ϵ_{c0} to ϵ_{c1}, and is equal to 1 when $\epsilon < \epsilon_{c1}$ (for strong compressive strains). Since ϕ is uniquely determined by the strain ϵ, so is the stress $\sigma = \mu(\epsilon - \epsilon_r(\phi))$. Our two-phase model thus behaves as a non-linear elastic material with a certain stress-strain response.

As shown in Figure 1a, this response is non-monotonic, and the phase transitions in our model are equivalent to mechanical instabilities in an elastic material with a non-monotonic stress-strain curve [35]. The states for which the slope is negative, which correspond to values of the phase intermediate between 0 and 1, are unstable. If the system is subjected to increasing strain, it deforms uniformly until $\epsilon = \epsilon_{c0}$, then phase-separates. When the two phases coexist, the stress has a fixed 'plateau' value σ_p, as do the strains in the two phases (see Figure 1a). In a biological context, the plateau stress can be understood as a 'homeostatic stress' restored by the formation of a collapsed region. If the strain is further increased, the proportion of the collapsed phase increases until the system is entirely collapsed, after which the strain is uniform again. Note that states intermediate between the plateau stress and the
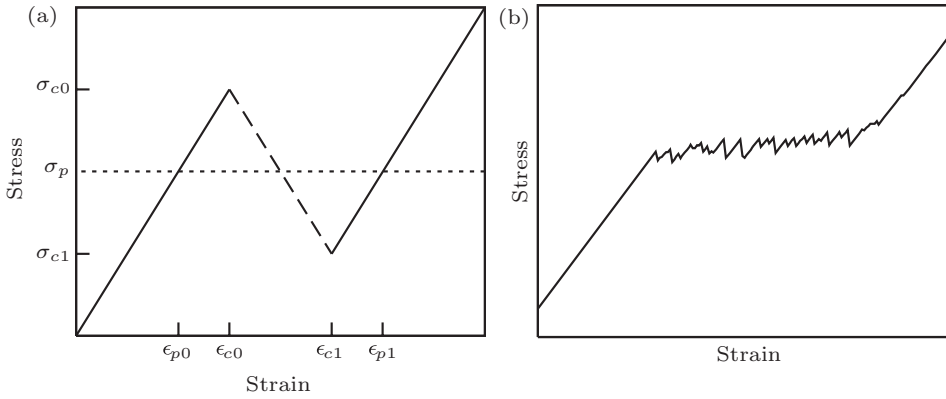
Figure 1. (a) Sketch of the stress-strain curve of the model. The dashed segment corresponds to unstable states, which phase-separate. The dotted horizontal line indicates the plateau stress observed when the two phases coexist. (b) Stress-strain response of a simulated inhomogeneous system.
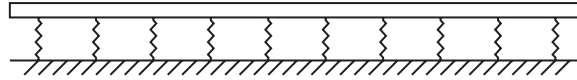

Figure 2. Diagram of the system. A layer of tissue (top) is coupled to a rigid substrate (bottom).

instability threshold are metastable, and in actual physical systems, the distinction between the two can be blurred by disorder [4]. This can be reproduced in our model by adding a random prefactor $r(x)$ to the terms $e(\phi, \epsilon) + f(\phi)$ in the expression of the energy (Equation (3)). This creates local weak spots, so that the collapsed phase nucleates before the critical stress for an ideal, homogeneous system (compare Figures 1a and b).

As illustrated by the simple, piecewise linear stress-strain curve shown in Figure 1a, our model provides a minimal description of a mechanism for the release of mechanical stresses by localized deformation. There are just enough parameters to allow independent adjustment of the properties that will determine its pattern-forming behavior, i.e. the instability threshold, the amount of deformation associated with the collapse, and the equilibrium stress at the interface between the two phases.

In what follows, we consider the system shown in Figure 2, in which a layer of tissue described by the above model is coupled to a rigid substrate. If there is any mismatch between the two layers, mechanical stresses are induced in the tissue. Such a layered arrangement is commonly used to model various mechanical instabilities, e.g. the fragmentation of thin films [36,37], and can be likened with the layered structure of plant leaves [11], with the rigid substrate representing the epidermis.

The coupling between the two layers is described by a quadratic potential, which included into the energy (Equation (4)) yields

$$E = \int \left[\frac{D}{2}(\partial_x \phi)^2 + \frac{\mu}{2}(\epsilon - \epsilon_r(\phi))^2 + f(\phi) + \frac{k}{2}(u - \eta x)^2 \right] \mathrm{d}x. \tag{9}$$

The parameter k represents the strength of the coupling, and η is a measure of the mismatch between the two layers, defined by $2L_s = (1 + \eta)2L$, where the $2L_s$ and $2L$ are the lengths of the substrate and of the tissue layer in an unstressed state.

To understand how the phase transition can be triggered, it is useful to compute the strain field when the tissue is in its initial state ($\phi = 0$).[3] The equation of mechanical equilibrium (Equation (1)) yields

$$\mu \partial_{xx} u - k(u - \eta x) = 0, \tag{10}$$

which is linear in u and admits solutions of the form

$$u = \eta x + A e^{x/\lambda} + B e^{-x/\lambda}. \tag{11}$$

In this equation, $\lambda = \sqrt{\mu/k}$ is a characteristic elastic length scale of the system, and A and B are constants that are determined by the boundary conditions. Here, the edges of the tissue are free of stresses, and $\partial_x u = 0$ at $x = \pm L_s$. Computing A and B and deriving Equation (11) with respect to x, we find that the strain in the tissue is given by

$$\epsilon = \eta \left(1 - \frac{\cosh(x/\lambda)}{\cosh(L_s/\lambda)} \right). \tag{12}$$

If the system is large compared to the elastic length scale λ, the strain is close to the strain imposed by the substrate everywhere except at the edges, and the stresses exhibit a broad plateau. If the system size is comparable to or smaller than the elastic length scale, the stresses have a more localized maximum at the center of the system, and the value of this maximum increases with the size of the system.

One way instabilities can be induced is by increasing the mismatch between the two layers (this is analogous to the situation of a shrinking film on a substrate). From the above, it appears that instabilities can also be induced by growth with the mismatch between the two layers being fixed, that is a result of uniform growth. The latter regime will always be considered when simulating patterning in growing tissues.[4]

We now turn to a numerical analysis of the evolution of the system. So far, we specified only its energy, which determines its states of equilibrium and their stability. To determine the new state of equilibrium reached after an instability occurs, its dynamics must be specified. A reasonable assumption is that mechanical relaxation is much faster than the transition between the two states of the tissue, so that at any time the system is at mechanical equilibrium:

$$0 = \frac{\delta E}{\delta u} = -\mu \partial_x (\partial_x u - \epsilon_r(\phi)) + k(u - \eta x). \tag{13}$$

Dynamics need thus be specified only for the phase field. We assume the latter obeys a relaxation equation of the form

$$\partial_t \phi \sim -\frac{\delta E}{\delta \phi} = D \Delta \phi - \partial_\phi e - \partial_\phi f. \tag{14}$$

At each time step of the overall evolution of the system, i.e. of its growth, this relaxation equation is solved assuming the system is at mechanical equilibrium, until an equilibrium is reached.[5] And this state of equilibrium satisfies the equations:[6]

$$\begin{cases} 0 = \mu \partial_x (\partial_x u - \epsilon_r(\phi)) - k(u - \eta x) \\ 0 = D \Delta \phi - \partial_\phi e - \partial_\phi f. \end{cases} \tag{15}$$

Most of the time, no instability occurs, and the new state of equilibrium is very close to the previous one. If an instability occurs, the phase field evolves to a new state that contains a different number of collapsed regions. Figure 3 shows a typical equilibrium configuration.

The results obtained in various conditions are shown in Figure 4. In the first example (Figure 4a), the tissue has a fixed size and the mismatch between the two layers is progressively increased. A limited number of collapsed regions are formed and grow to occupy the entire tissue. In the second example (Figure 4b), the system grows with the mismatch remaining constant ($L = e^{t/\tau} L_0$ and $L_s = e^{t/\tau} L_{s0}$). In that case, instabilities occur with time in an approximately self-similar cascade. Note that in both of these examples, the existing collapsed zones readjust after each new instability, and the system relaxes to a regular pattern that minimizes its energy. In the process, existing collapsed zones may change size or position, which is possible because the transition between the phases is reversible. In the case of a growing system (Figure 4b), this means that the pattern does not retain any trace of the history of its formation.

Now, if the transition to the collapsed state represents tissue differentiation, it should be irreversible, precluding the above rearrangements. A simple way of implementing irreversibility is to make the evolution of the phase field ϕ irreversible. Assuming that the transition must progress to a certain point before it becomes
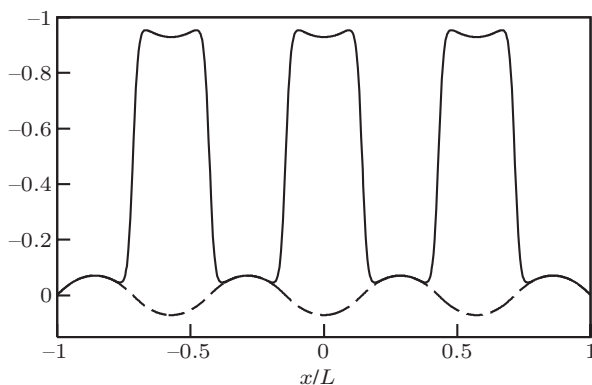

Figure 3. A simulated pattern with three collapsed zones. The solid line and the dashed line represent the strain and the stress, respectively. The parameters of the model are $\mu = 1$, $\epsilon_{r1} = -1$, $\alpha = -0.25$, $\beta = 0.25$, $D = 4 \times 10^{-4}$, $k = 16$, $L = 1$, and $\eta = -0.5$. With these values, the elastic length scale is $\lambda = 0.25$, the instability threshold is $\epsilon_{c0} = -0.25$ and the plateau stress is $\sigma_p = 0$. Accordingly, the strains in the two phases when they coexist are equal to the rest strains in their rest configurations, i.e. $\epsilon_{p0} = 0$ and $\epsilon_{p1} = -1$.
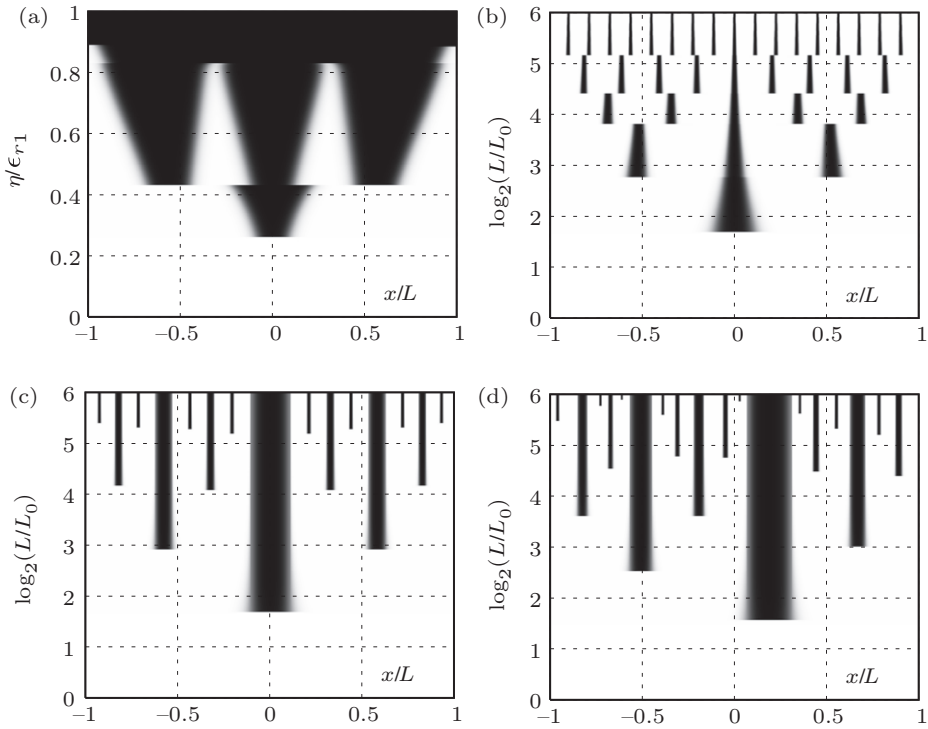
Figure 4. Patterns obtained in a one-dimensional system. These plots show the evolution of the phase field, with the collapsed regions appearing in black. Model parameters are given in Figure 3. (a) Increasing mismatch between the two layers, with the size of the tissue being fixed ($L = 1$). (b)–(d) Growing system with a fixed mismatch ($\eta = -0.275$). The initial size of the tissue is $L_0 = 0.25$. (b) Reversible evolution. Note that the collapsed regions appear to shrink only because the total size of the system increases. (c) Irreversible evolution. (d) Same as (c) with disorder.

irreversible, we allow ϕ to increase or decrease when it is smaller than a certain threshold ($1/2$), and only to increase when it is larger.[7] As shown in Figure 4c, this yields hierarchical patterns, which reflect the history of the system. The collapsed zones grow along with the system, so that earlier-formed zones are larger than more recent ones.

So far, we assumed that the tissue was perfectly homogeneous, and it may be of interest to examine how disorder, which is inherent in biological tissues, would affect the outcome of the model. As described earlier, disorder can be incorporated as a multiplicative noise term in the energy of the system. Instabilities then no longer occur exactly at the locations where the stresses are largest. Figure 4d shows an example of the resulting irregular patterns. Consistent with theoretical arguments and experimental results concerning crack patterns [37,38], we find that the effect of disorder depends crucially on how the distance between collapsed regions compares with the elastic length scale λ. If this distance is much larger than λ, then the stresses exhibit a broad plateau and the location of new collapsed zones is very variable, being governed essentially by the weak spots due to disorder. On the other hand,

if the distance between the collapsed regions is comparable to or smaller than λ, then the stresses have a more localized maximum and the location of new collapsed zones is close to the location of this maximum. The latter regime is thus more favorable for obtaining regular and reproducible patterns. It is worth noting that in growing plant leaves, the distance between veins is of the same order as the thickness of the leaf [16] (which sets the characteristic length scale for elastic coupling between veins).

3. Two-dimensional model

We now turn to the extension of the model to two-dimensional systems. In this context, the one-dimensional patterns described in the previous section can be interpreted as parallel stripes of localized deformation. The more general patterns that we expect to describe would take the form of networks of stripes of different orientations, corresponding to different principal directions of deformation. It is thus clear that a scalar parameter is no longer sufficient to describe the collapsed state. Since the difference between the two phases lies only in their rest configurations, we choose here to identify the phase field ϕ and ϵ_r, which in 2D is a tensor describing the local rest configuration. Likewise, the mismatch between the two layers is now described by a tensor η. The 2D analog of Equation (9) thus takes the form

$$E = \int \left[\frac{D}{2} |\nabla \epsilon_r|^2 + \frac{\lambda}{2} \text{Tr}(\epsilon - \epsilon_r)^2 + \mu |\epsilon - \epsilon_r|^2 + f(\epsilon_r) + k(\mathbf{u} - \eta \mathbf{x})^2 \right] dS. \qquad (16)$$

While η may be anisotropic, we assume that the tissue has no preferential direction. Accordingly, f can be expressed as a function of the invariants of ϵ_r, e.g. its trace and its norm.

To obtain a behavior similar to that of the one-dimensional model, we consider potentials that have a minimum for $\epsilon_r = 0$ and a minimum of the same depth for values of ϵ_r corresponding to a smaller natural volume (i.e. $\text{Tr}\epsilon_r < 0$). Among all possible potentials satisfying this constraint, we have chosen the following three illustrative examples. In the first, the secondary minimum is reached for all deformations having a given amplitude (norm), regardless of the shear. The second one specifically favors uniaxial deformations. In contrast, the third one has a secondary minimum for isotropic compression.

More specifically, the first potential is defined by

$$f(\epsilon_r) = -(|\epsilon_r| - 1/2)^2 + (|\epsilon_r| - 1/2)^4, \qquad (17)$$

which has minima for $\epsilon_r = 0$ and for $|\epsilon_r| = 1$ (see Figure 5a). The second and third examples are defined as polynomials of the invariants of ϵ_r, i.e.

$$f(\epsilon_r) = \sum c_{ij} (\text{Tr}\,\epsilon_r)^i |\epsilon_r|^{2j}. \qquad (18)$$

The two sets of coefficients used are $c_{20} = 0.4$, $c_{01} = 0.2$, $c_{30} = 0.7$, $c_{11} = 0.5$, $c_{40} = 0.4$, $c_{21} = 0.1$, $c_{02} = 0.1$, which corresponds to minima for uniaxial deformations (see Figure 5b) and $c_{20} = 0.25$, $c_{01} = 0.5$, $c_{30} = 1$, $c_{11} = 0$, $c_{40} = 0.375$, $c_{21} = 0$, $c_{02} = 0.5$, which leads to a minimum for isotropic compression (see Figure 5c).[8]
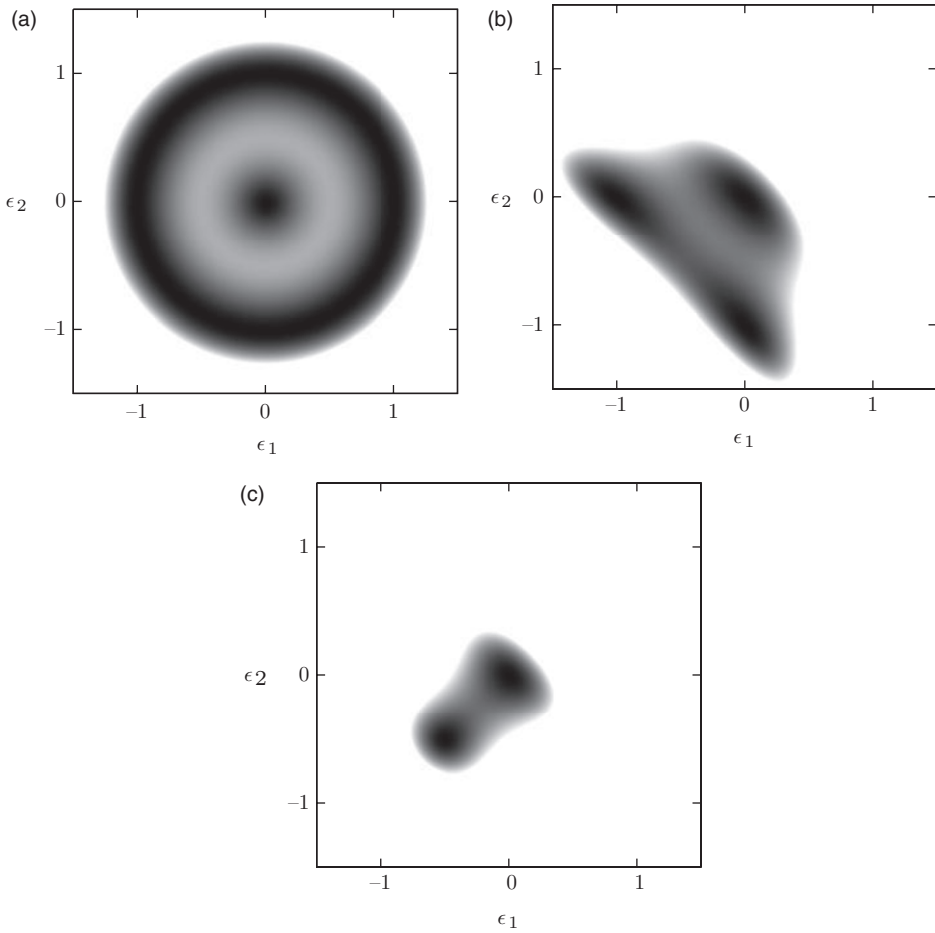
Figure 5. Gray scale plots of the different potentials $f(\epsilon_r)$ used. ϵ_1 and ϵ_2 are the eigenvalues of ϵ_r. Darker regions correspond to lower values. (a) The potential defined by Equation (17) favors compressive strains of a given amplitude, regardless of the shear. (b) The potential defined by Equation (18) and the first set of coefficients given in the text favors uniaxial compression. (c) The potential defined by Equation (18) and the second set of coefficients favors isotropic compression.

In contrast to the one-dimensional system shown in Figure 2, in which the edges were free of stresses, most of the 2D simulations were done with periodic boundary conditions, which allow the mechanical equilibrium equation to be efficiently solved in Fourier space. In this case, the phase field is initially chosen to be random, to break the symmetry of the system. The initial conditions (mismatch or size for a growing system) are chosen such than an instability immediately develops, preventing relaxation to a uniform state.

As in the one-dimensional case, we first consider reversible evolution in a non-growing system (Figure 6). Here, the mismatch between the two layers is directly set to its final value, and the system is allowed to relax to equilibrium. The first two
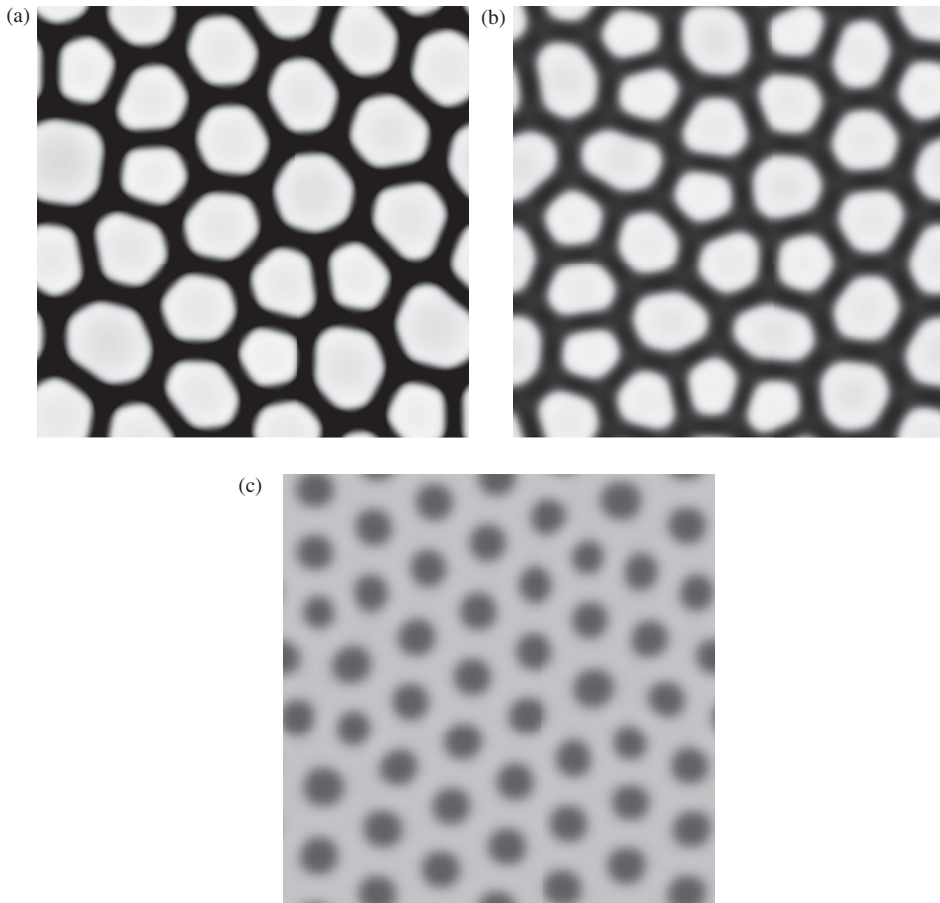
Figure 6. Typical patterns observed in a layered two-dimensional system with the different potentials. Periodic boundary conditions were used and the initial state was randomly perturbed. Gray levels correspond to the trace of the rest configuration ϵ_r, with darker areas corresponding to collapsed regions. Potentials that allow or favor uniaxial compression (a) and (b), corresponding to the potentials of Figures 5a and b, respectively) yield reticulate patterns, while the potential that favors isotropic compression produces discontinuous domains arranged in a hexagonal lattice (c), corresponding to the potential of Figure 5c).

potentials (shown in Figures 5a and b), which allow or favor uniaxial compression, yield very similar patterns of interconnected stripes, which could be likened to crack networks in directional growth systems such as basalt columns [39]. In contrast, the potential shown in Figure 5c, which favors isotropic compression, produces islands of localized deformation arranged in an hexagonal lattice, which are similar to some structures observed in solid-solid phase transitions [27]. The characteristic length of the above patterns, as in 1D, is set by the elastic length scale $\lambda = \sqrt{\mu/k}$.

The difference between the two potentials that produce reticulate patterns becomes more apparent when considering a growing system (and a reversible evolution), which makes it possible to observe individual nucleation events leading to

the formation of new collapsed regions. Indeed, in the case of the potential of Figure 5a, new collapsed regions take the form of trijunctions that split an uncollapsed region into three,[9] while in the case of the potential of Figure 5b, they occur as single stripes that divide an uncollapsed region across its longest extension.[10] This qualitative difference can be explained by the fact that the core of a trijunction is compressed in both directions, a state that is disfavored by the potential of Figure 5b.

Finally, we consider irreversible evolution in a growing system, which we found to lead to hierarchical patterns in 1D. In that case, irreversibility was implemented by forcing the evolution of the scalar phase field to be monotonic once a certain threshold was exceeded. A straightforward extension to two dimensions would be to apply the same rule to the trace of the rest configuration tensor ϵ_r. However, this would allow the principal directions of the rest configuration in the collapsed phase to vary (and simulations indicate that this can indeed occur). Instead, we wish the establishment of these special directions to be definitive, as is the transition to the collapsed state (think of the elongation of vascular cells in plant leaves). Accordingly, we impose that, once the compression in some direction has exceeded a certain threshold, it can no longer decrease.[11]

As in 1D, we consider a growing system with a fixed mismatch, and find that hierarchical structures are obtained. As shown in Figure 7, the shape of the patterns depends both on the potential used and on the shape of the growing domain (for the earliest structures that are formed). However, we find that the simple model presented here produces unexpected artifacts, such as regions of lower compression within the collapsed zones, and open-ended collapsed regions that fail to reconnect with previously formed structures.

As illustrated by Figure 8, these effects are caused by tensions that accumulate in the collapsed structures as they grow. When the transition to the collapsed state is reversible, the collapsed regions tend to an equilibrium width such that compressive stresses are relaxed in their neighborhood (i.e. for an ideal, infinitely long and straight stripe, the stress at the interface has a fixed value equivalent to the plateau stress σ_p of the one-dimensional model). In contrast, in the irreversible case, the width of each collapsed region grows along with the system and exceeds its equilibrium width. Instead of just releasing the compression in their vicinity, these growing collapsed regions give rise to tensile stresses. As can be seen in Figure 7, these tensile stresses both destabilize the collapsed regions, and prevent the progression of new collapsed regions towards them. It must be noted that such tensile stresses are also generated in the 1D model. However, they do not have such dramatic effects in that case, because new collapsed structures always form away from existing ones.

4. Discussion

In this article, we explored a possible mechanism for biological patterning by mechanical stresses. This mechanism, which involves the stress-mediated transition of a tissue between two states, was shown to yield a response similar to that of a non-linear elastic material, justifying an analogy with mechanical instabilities.
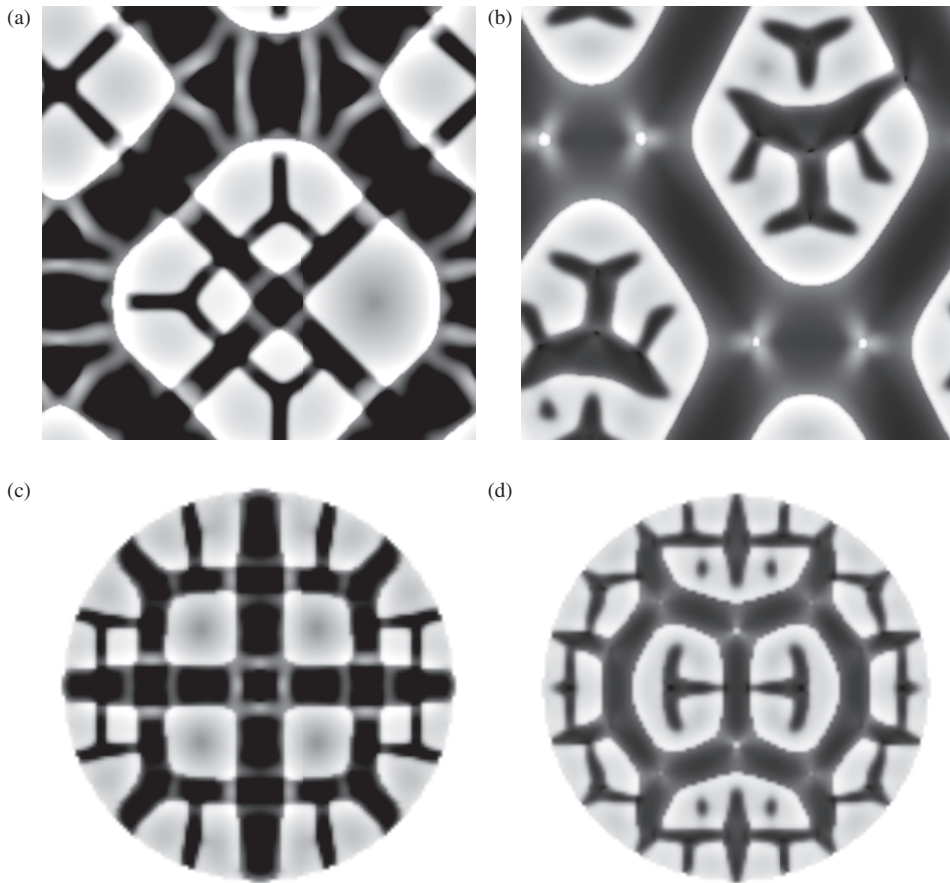
Figure 7. Patterns generated by irreversible evolution in growing systems with different potentials and boundary conditions (periodic boundary conditions or circular domains). (a) and (c) were obtained with the potential of Figure 5a, (b) and (d) with the potential of Figure 5b. As expected, hierarchical structures are formed. However, they are disrupted by the tensions that accumulate within and around the collapsed regions as they grow (see text and Figure 8). Notice the lighter spots or stripes within the collapsed regions.

The formation of patterns was driven by coupling the tissue to a rigid substrate, which could represent a stiffer tissue such as the epidermis of plant leaves. As in the mechanical instabilities of layered physical systems, such as the wrinkling of a film bound to a substrate, this elastic coupling introduces a characteristic length scale that governs the size of the patterns.

We first analyzed a one-dimensional system. In this case, the model involves a small number of parameters, and it is possible to describe the equilibrium patterns analytically. Numerical simulations showed that regular patterns, which are largely independent of the history of the system, are obtained when the transition between the two states of the tissue is reversible. In contrast, when this transition is made irreversible to represent tissue differentiation, the history of the system is retained in
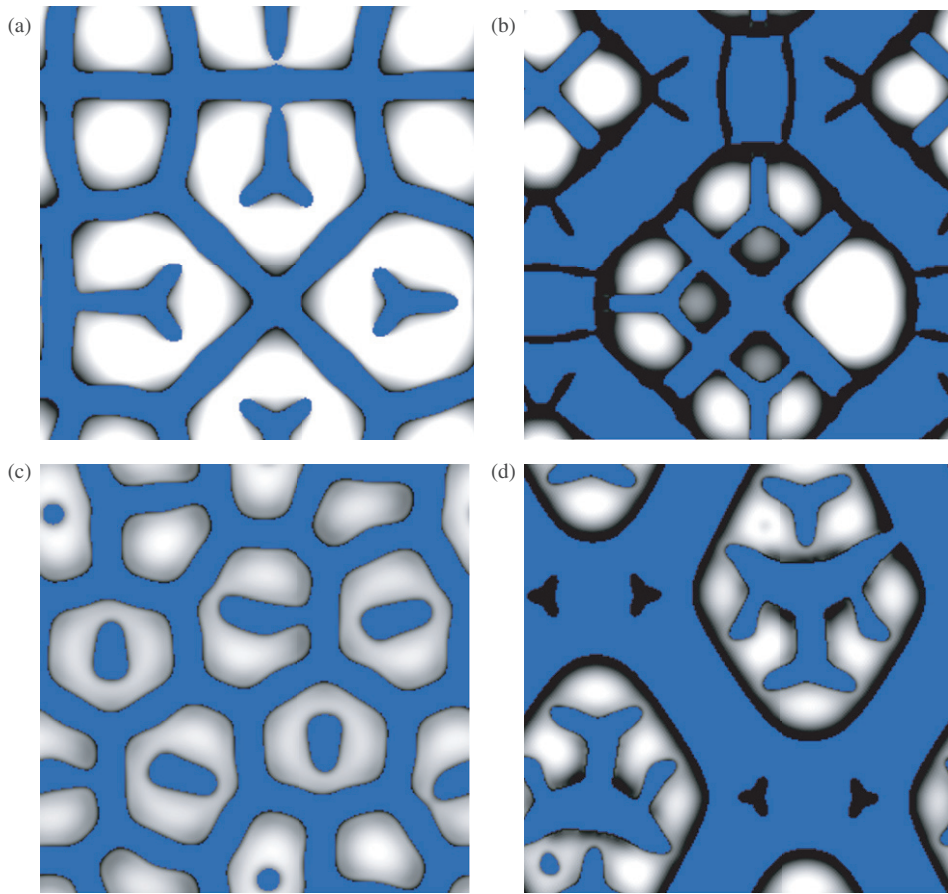
Figure 8. (Color online). Effect of irreversibility on the mechanical state of the system and pattern formation. All figures represent growing systems with periodic boundary conditions. (a) and (b) were obtained with the potential of Figure 5a, (c) and (d) with the potential of Figure 5b. Evolution was reversible in (a) and (c), irreversible in (b) and (d). Collapsed regions (defined by thresholding the value of $\mathrm{Tr}(\epsilon_r)$) are shown in blue (online). Gray levels indicate compressive stresses (lighter regions are more strongly compressed), and regions appearing in black are under tension. In the reversible case, the stresses decrease near the collapsed regions, yet generally remain compressive. In the irreversible case, this is also true for recently formed structures. In contrast, the larger, older structures generate tensile stresses. These tensile stresses hinder the progression of newly formed structures, yielding disconnected patterns.

its final state. In a growing system, new structures keep forming over time, yielding hierarchical patterns. This is very similar to the development of leaf venation networks, in which veins of different orders form successively over the course of leaf growth [16].

In two dimensions, because of the tensorial nature of elastic fields, the potential that characterizes the preferred states of the tissue can have many different forms. While we did not carry out a systematic analysis, the different examples considered suggest that reticulate patterns can readily be obtained when the potential allows or

favors uniaxial deformations of the tissue. In contrast, islands of deformed tissue are obtained with a potential that favors isotropic deformations. This suggests that a mechanical model of leaf venation patterning could account for both wild-type patterns and the disconnected vasculature observed in certain mutants [40].

A very similar model of leaf vein patterning was recently proposed in [17]. In that approach, however, the different states of the tissue are characterized by a single scalar order parameter. The transition to the collapsed state is associated with an isotropic deformation, and the collapsed tissue is assumed to have a reduced shear modulus to allow the formation of reticulate patterns. The elongation of vascular cells is described as a change of their rest volume combined with a strong elastic shear. One benefit of this approach is that it involves a much smaller number of parameters. However, it is unclear that it gives a realistic description of the mechanical state of vascular cells. While it comes at the cost of a greater complexity, we find it more appropriate to describe the elongation of vascular cells as a change in their rest shapes. This also makes it possible to address the effect of variations in these rest shapes on the overall pattern. For instance, as mentioned above, our results suggests that failure to elongate properly can lead to disconnected patterns such as are observed in some mutants.

From the preceding results, we expected that the introduction of irreversibility in a growing two-dimensional system would lead to hierarchical, reticulate patterns. However, we found that strong tensile stresses develop in collapsed regions as they grow beyond their initial, equilibrium size, and dramatically affect the evolution of the system. This is a consequence of the very simple growth laws assumed in our model. The rest configuration of the tissue changes when it switches between its two states, but growth in each of the two states is uniform and proceeds at a constant rate, allowing residual stresses to accumulate. In reality, the growth of biological tissues depends on the mechanical stresses to which they are subjected [41,42], which can be expected to limit the buildup of residual stresses. Incorporating this dependence would be essential to further investigate biological patterning by mechanical forces. Another perspective would be to integrate the mechanical approach developed here with the biochemical factors of tissue differentiation. For instance, the differentiation of vascular cells in plant leaves involves the expression and polar localization of auxin carrier proteins [13], and it would be of interest to investigate how these processes are connected with the elongation of vascular cells.

Notes

1. Conversely, localized deformation in non-linear elastic materials can be interpreted as a first-order phase transition.
2. The parameters are chosen such that the critical strains defined below satisfy $\epsilon_{c1} < \epsilon_{c0}$.

3. Similar calculations could be carried out for the states of equilibrium in which the two phases coexist if the width of the interfaces is neglected.
4. If the two layers were instead assumed to grow at different rates, then the mismatch would become arbitrarily large with time.
5. The equations of mechanical equilibrium (a set of linear equations) are solved at each step of the relaxation. The relaxation is stopped when the rate of change of the phase field falls below a certain threshold.
6. We are thus assuming that there are three well separated time scales $\tau_{\text{mech}} \ll \tau_{\text{diff}} \ll \tau_{\text{growth}}$, where τ_{mech}, τ_{diff}, and τ_{growth} are the characteristic time scales corresponding to mechanical relaxation, cell differentiation, and growth, respectively.
7. Such an *ad hoc* rule would clearly be unsatisfactory to describe a physical system, but in the case of biological systems, it can be seen as a necessary simplification of the complex phenomena involved.
8. Note that the potential defined by Equation (17) cannot be written in this form.
9. A typical example in the case of an irreversible evolution can be seen in Figure 8a.
10. A typical example in the case of an irreversible evolution can be seen in Figure 8c.
11. To this end, we define a 'maximum deformation tensor' ϵ_m that keeps track of the maximum past compression in any direction, i.e. the tensor $\epsilon_r(t) - \epsilon_m(t')$ is positive for all times $t < t'$. From this maximum deformation tensor, we define an 'irreversible deformation tensor' ϵ_i. In a basis that diagonalizes ϵ_m, $\epsilon_i = \text{diag}(f(\lambda_1), f(\lambda_2))$, where $\epsilon_m = \text{diag}(\lambda_1, \lambda_2)$. The function f is defined by $f(x) = 0.9x$ if $x < -0.5$ and $f(x) = \infty$ if $x > -0.5$, so that compressions in excess of 0.5 are stored in ϵ_i. Irreversibility is implemented by imposing that the tensor $\epsilon_r - \epsilon_i$ is negative. The factor 0.9 in the definition of f was introduced to prevent numerical instability.

References

[1] L.B. Freund, *Dynamic Fracture Mechanics*, Cambridge University Press, Cambridge, 1990.
[2] E. Cerda and L. Mahadevan, Phys. Rev. Lett. 90 (2003) p.074302.
[3] B. Audoly, Phys. Rev. Lett. 83 (1999) p.4124.
[4] G. Gioia, Y. Wang and A.M. Cuitino, Proc. R. Soc. A 457 (2001) p.1079.
[5] M. Ben Amar and A. Goriely, J. Mech. Phys. Solid. 53 (2005) p.2284.
[6] E. Sharon, B. Roman and H.L. Swinney, Phys. Rev. E 75 (2007) p.046211.
[7] T. Lecuit and P.F. Lenne, Nat. Rev. Mol. Cell Biol. 8 (2007) p.633.
[8] E. Farge, Curr. Biol. 13 (2003) p.1365.
[9] C.M. Nelson, R.P. Jean, J.L. Tan, W.F. Liu, N.J. Sniadecki, A.A. Spector and C.S. Chen, PNAS 102 (2005) p.11594.
[10] L. Hufnagel, A.A. Teleman, H. Rouault, S.M. Cohen and B.I. Shraiman, PNAS 104 (2007) p.3835.
[11] Y. Couder, L. Pauchard, C. Allain, M. Adda-Bedia and S. Douady, Eur. Phys. J. B 28 (2002) p.135.
[12] T. Sachs, Adv. Bot. Res. 9 (1981) p.151.
[13] E. Scarpella, D. Marcos, J. Friml and T. Berleth, Gene. Dev. 20 (2006) p.1015.
[14] F.G. Feugier, A. Mochizuki and Y. Iwasa, J. Theor. Biol. 236 (2005) p.366.
[15] V. Fleury, J.F. Gouyet and M. Léonetti (eds.), *Branching in Nature*, Springer, Berlin, 2001.
[16] T. Nelson and N. Dengler, Plant Cell 9 (1997) p.1121.
[17] M.F. Laguna, S. Bohn and E.A. Jagla, PLoS Comput. Biol. 4 (2008) p.e1000055.
[18] J.B. Collins and H. Levine, Phys. Rev. B 31 (1985) p.6118.
[19] A. Karma and W.J. Rappel, Phys. Rev. E 57 (1998) p.4323.

[20] G.J. Fix, in *Free Boundary Problems: Theory and Applications*, N. Niezgódka and S. Streelecki, eds., Pitman, London, 1983, p.580.

[21] J.S. Langer, *Model of pattern formation in first order phase transitions*, in *Directions in Condensed Matter Physics*, G. Grinstein and G. Mozenko, eds., World Scientific, Singapore, 1986, p.165.

[22] W.J. Boettinger, J.A. Warren, C. Beckermann and A. Karma, Annu. Rev. Mater. Res. 32 (2002) p.163.

[23] R. González-Cinca, R. Folch, R. Benítez, L. Ramírez-Piscina, J. Casademunt and A. Hernández-Machado, *Phase field models in interfacial pattern formation out of equilibrium*, in *Advances in Condensed Matter and Statistical Physics*, E. Korutcheva and R. Cuerno, eds., Nova, 2004, p.203.

[24] R. Folch, J. Casademunt, A. Hernández-Machado and L. Ramírez-Piscina, Phys. Rev. E 60 (1999) p.1724.

[25] T. Biben and C. Misbah, Phys. Rev. E 67 (2003) p.031908.

[26] Y. Wang, L.Q. Chen and A.G. Khachaturyan, Acta Metall. Mater. 41 (1993) p.279.

[27] Y. Le Bouar, A. Loiseau and A.G. Khachaturyan, Acta Mater. 46 (1998) p.2777.

[28] T. Pusztai, G. Bortel and L. Gránásy, Europhys. Lett. 71 (2005) p.131.

[29] R. Kobayashi and J.A. Warren, Physica A 356 (2005) p.127.

[30] A. Karma, D.A. Kessler and H. Levine, Phys. Rev. Lett. 87 (2001) p.045501.

[31] H. Henry, Europhys. Lett. 83 (2008) p.16004.

[32] H. Henry and H. Levine, Phys. Rev. Lett. 93 (2004) p.105504.

[33] R. Spatschek, M. Hartmann, E. Brener, H. Muller-Krumbhaar and K. Kassner, Phys. Rev. Lett. 96 (2006) p.015502.

[34] D. Pilipenko, R. Spatschek, E.A. Brener and H. Muller-Krumbhaar, Phys. Rev. Lett. 98 (2007) p.015503.

[35] J.L. Ericksen, J. Elasticity 5 (1975) p.191.

[36] P. Meakin, Thin Solid Films 151 (1987) p.165.

[37] O. Morgenstern, I.M. Sokolov and A. Blumen, J. Phys. A 26 (1993) p.4521.

[38] S. Bohn, J. Platkiewicz, B. Andreotti, M. Adda-Bedia and Y. Couder, Phys. Rev. E 71 (2005) p.046215.

[39] K.A. Shorlin, J.R. de Bruyn, M. Graham and S.W. Morris, Phys. Rev. E 61 (2000) p.6950.

[40] K. Koizumi, M. Sugiyama and H. Fukuda, Development 127 (2000) p.3197.

[41] K.P. Barley, J. Exp. Bot. 13 (1962) p.95.

[42] S.C. Cowin, Annu. Rev. Biomed. Eng. 6 (2004) p.77.